Journal of Engineering Science and Technology
Vol. 17, No. 1 (2022) 0552 - 0562

PARAMETERS FOR FE_2O_3 ON STAPHYLOCOCCUS AUREUS AND ACINETOBACTER BAUMANNIL

B. M. AHMED[1,*], R. A. ABDULRAZAQ[2],
M. A. KHALAF[1], O. A. A. DAKHIL[1]

[1]Department of physics, College of Science, Mustansiriyah University, Iraq
[2]Department of biology, College of Science, Mustansiriyah University, Iraq
*Corresponding Author: dr.baida_222@uomustansiriyah.edu.iq

Abstract

Plasma energy is used to enhance the antibacterial properties of a Fe_2O_3 nanoliquid on Staphylococcus aureus and Acinetobacter baumannii. Fe_2O_3 plasma was produced using laser-induced plasma spectroscopy (LIPS) technique with a wavelength of 1064 nm. Spectral irradiation was conducted with a pulsed laser at different energies (600–900 mJ) under ambient conditions in air. The electron temperature was determined at different peak laser powers using the Boltzmann (-1/K_B T) and Saha equations, and the electron density was deduced from the Stark broadening. The effect of the iron oxide on the intensity of the emission lines and plasma parameters is discussed. Electron temperatures of Fe_2O_3 were measured in the range of 1.66–2.4 eV. We observed an effect due to Fe_2O_3 at 800 mJ against Staphylococcus aureus and Acinetobacter baumannii with inhibition zones of 30 mm and 23 mm, respectively, but no effect was observed for either bacteria at 600 or 700 mJ on either type of bacteria.

Keywords: Inhibition bacteria, Iron and iron oxide plasma, Laser induced plasma spectroscopy, Plasma parameters.

1. Introduction

Laser-induced plasma spectroscopy (LIPS) has recently been used for the spectrophysical analysis of biological samples such as bacteria, bone, microorganisms and tissues. The spectroscopy technique has many applications in the biomedical sciences, of which the identification of pathogenic bacteria is an important one. LIPS is a rapid diagnostic that could confirm the presence of bacteria and diagnose the species or strain [1].The spectrum emission from a plasma Equipped information about the plasma parameters, where Laser-induced Breakdown Spectroscopy (LIBS) used to calculate different parameters, as electron density (ne), electron temperature (Te) and plasma frequency (f_p). To expect the (OES) the spectral emission from plasma must be studied. [1]. Optical emission spectroscopy (OES) as a flexible technique and easy method to diagnostics the parameters with an easy experimental setup. The radiations emitted from plasma take place by collisions laser spectral with atoms, molecules, and causes to excited them, and analyzed the spectral by spectroscopy [2-4].

The spread and development of intense lasers have allowed creating easy tools and good techniques for the control of electronic motions in different forms of matter (gas, liquid, solid, and plasma). These techniques at the same time provide direct information about spectral lines and a wide range of collisions electron phenomena (energy, density, thermal and other information) [5, 6].

The Boltzmann plot is a basic method to expect and estimate the electron temperature in plasma by imposing that the plasma condition is in a state of thermodynamic equilibrium a reason to high collisions between particles and incident laser [6, 7]. Saha - Boltzmann distribution is the best method to evaluate the atomic transitions for upper levels. Where suppose the excitation and electron temperatures are same [8].

There are two reasons theoretically study plasma and optical properties. One understands the phenomenon of collisions between electrons and atoms in the plasma and evolution of the parameters generated and analytical spectral lines. The other reason is related to the search for absolute analysis by laser-induced plasma spectroscopy (LIPS) [9, 10].

LIPS one of the most important techniques to study the more biological applications such as inhibition bacteria, it's a very small organism. The size of bacteria between 0.3 µm and 5µm, divided in two groups relies on cell wall, Gram-positive and Gram-negative bacteria, cell wall of Gram-negative bacteria features a porous outer membrane into the outer surface of which the lipopolysaccharide responsible for the pathogenesis of Gram-negative infections is integrated. The cell wall of Gram-negative bacteria does not possess such an outer membrane. Its murein layer is thicker and contains teichoic acids and wall associated proteins that contribute to the pathogenic process in Gram-positive infection [11].

Spectroscopic is the best dives to estimate the data generated by plasma, by the line intensities and their ratio between two lines which reflect of neutral or ionic excited. The more relevant parameters are the plasma frequency, f_p, temperature, T_e, and electron density, n_e. We can estimate the plasma temperature from the Boltzmann and Saha equations and calculated from Eq. (1) [12, 13]

$$T_e = \frac{E_1 - E_2}{k_B ln\left(\frac{\lambda_2 I_2 g_1 A_1}{\lambda_1 I_1 g_2 A_2}\right)} \quad (1)$$

where $I, g, A\ and\ \lambda$ represent the intensity (Mw/cm^2), statistical weight, absorption oscillator strength and wavelength, and E is the excitation energy of one state in (eV), and k_B is the Boltzmann constant.

The free electrons per unit volume can describe by Electron density. So, the spectral lines of an element can estimate by the Suha- Boltzmann equation of ionization stages. The equation is given as [14],

$$n_e = \frac{I_1}{I_2^*}\ 6.04 \times 10^{21} (T)^{3/2}\ e^{\left(\frac{-E_k - E_i - x_z}{KT}\right) \times T_e^{3/2}} \quad (2)$$

where (E_k, E_i) is the energy for levels (1 and 2) gives a straight line with slope equal to Eq. (1). The plasma temperature can determine by graph slope.

The ionization energy of atoms in (cm^{-3}) Fe_2O_3 targets we can get from,

$$I_2^* = \frac{I_2 \lambda_2}{g_2 A_2} \quad (3)$$

where g_2 represents the statistical weight of transition between two levels from level (2) to level (1), λ_2 is the wavelength of transition between two levels and A_2 is the probability of transition from level two to level one. So we calculated plasma frequency from Eq. (4) [15, 16],

$$f_p = \frac{n_e e^2}{m_e \varepsilon_0} \quad (4)$$

One of the most important plasma parameters is the plasma frequency [17]. The distance of the individual particle is that carries a reverse charge in the medium of plasma and represent the fundamental characteristic is the Debye length λ_D (cm), this parameter proportional directly with the square root of the electron temperature in inversely with electron density dependence to Eq. (5) [18, 19],

$$\lambda_D = \sqrt{\frac{\varepsilon_0 K_B T_e}{n_e e^2}} = 7430\ \left(\frac{T_e}{n_e}\right)^{1/2} \quad (5)$$

where n_e is the electron density (cm^{-3}), T_e is the electron temperature eV, (e =1.6×10^{-19} c). On the other hand, we can evaluate the number of particles in the Debye sphere, N_D, we are dependent on the density and temperature of the electron, Debye length or Debye sphere represents second condition to take place the plasma existence N_D>>1. The equation of Debye sphere is [20],

$$N_D = \frac{4}{3}\pi {\lambda_D}_D^3 n_e \quad (6)$$

A Debye sphere is an important parameter where represents the radius of the charges, the number of particles in a (Debye sphere) with a radius, equal to the Debye radius [21].

2. Experimental Analysis

2.1. Preparation and method

In this work used Fe_2O_3 by compaction of powders into a circular geometric form. Using iron powder and iron oxide powder with a purity of 99.99% as shown in Fig. 1(a), where take the weight (3 g) from every material and pressed per tablet of the

material as shown in Fig. 1(b), Pressing them usually performed at room temperature where the powder put inside a cylinder made of stainless steel and pressed by a hydraulic piston with a compressive strength of approximately 6 tons and the powder was converted into a disk (pellets) of Fe_2O_3 material so the thickness of the disk (5 mm and a diameter of 10 mm), which allows. Pressing is the best of the practice to reduce the size of the tablet and the air gaps that exist within a single disk.

The iron oxide employed for LIPS to analysis consists of particles and study the spectral emissions from them, different parameters estimate and evaluated as ne, , and . All these parameters study at a wavelength (1064 nm), to explain the effect same wavelength on the metal (Fe_2O_3). And appear the applications of them through the number of particles in Debye length, temperature, and density of electrons.

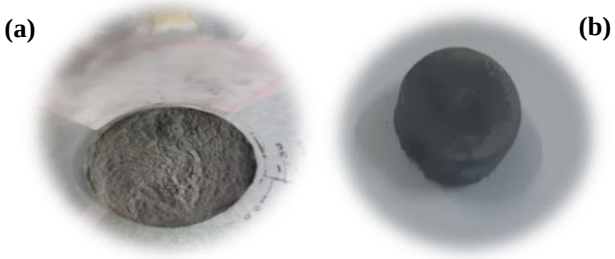

Fig. 1. Represent (a) Oxide Iron (Fe_2O_3) material with a purity of 99.99% before pressing. (b) (Fe_2O_3) material after pressing.

Use LIBS system Fig. 2 consists of a Q-switched Nd: YAG pulsed laser, wavelength (λ=1064) nm at different energies (600-900) mJ. To generate plasma incident on the metal and appear difference spectral lines with and without oxide, to get Accurate measurements during experimental and avoid delay mechanism spectrum of incident laser-generated plasma as excitation, use very accurate lens (200-2000) nm to focusing the laser beam, and in order not to take place any breakdown of air in front of the sample (Fe_2O_3), focusing lens and the sample was separated by a distance less than the focal length of the lens. Use optical fiber and put the fiber in 45^o to collecting and transfer plasma emission. Spectroscopy optics use to study the plasma emission (200-1025) nm.

Fig. 2. Spectroscopy Ocean Optics and optical fibre.

From Fig. 3 note the methods of incident laser on the solid targets (Fe_2O_3), where clear from this figure the system consists of (computer, spectroscopy, fiber,

laser, and targets), we see from plasma plume the intensity and volume of the (Fe_2O_3) are limited and increases with increasing the laser energy.

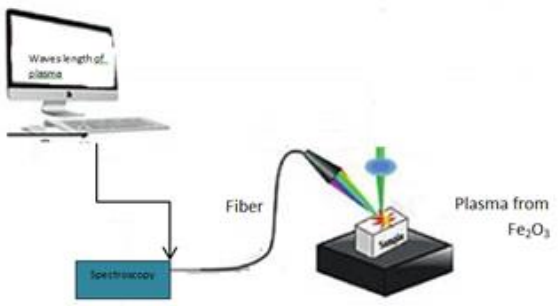

Fig. 3. Schematic diagram experimental of the spectroscopy optics and optical fibre.

3. Results and Discussion

In this section illustrate the typical emission spectrum plasma that generated from the incident laser beam on surface targets, Fe_2O_3 and compares between them through study, the best peak of wavelength, temperature, frequency, and density all these parameters under induced laser plasma technique.

The emission spectrum lines detected and analysed the intensities of it to evaluate the properties of plasma thorough electron temperature Eq. (1) and electron density Eq. (2) at different laser energies (600-900) mJ.

From Fig. 4, it is clear that the laser peak power has a strong and important effect on the emission line intensities, where the intensities increase with energy. Appear from figures the emission of spectral of iron oxide increases where the highest peak lies at (FII), wavelength 589.8 at peak 62672.95 and the transition 3d54s2 - 3d6(3D)4p, but when incident laser on Fe target finds the intensity becomes less and the highest peak lie at (FII), wavelength 591.37639 at peak 55396.52 and the transitions 3d6(3F2)4p - 3d6(5D)5s.

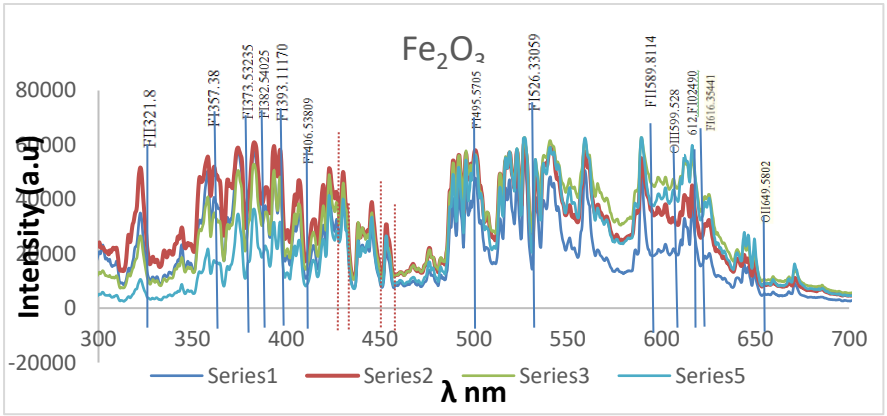

Fig. 4. Emission spectra of (LIPS) for Fe_2O_3 with different energies.

Table 1 illustrates the lines emissions from the Fe_2O_3 plasma excitations and ionizations that produced by the interaction of pulse Nd: YAG laser a wavelength (1064) nm with at different laser energies (600-900).

Table 1. Spectroscopic parameters of the (Fe_2O_3 I and Fe_2O_3 II) lines [22].

Ions	Wavelength λ (nm)	g_kA_{ki} (S^{-1})	E_i (cm^{-1})	E_k (cm^{-1})	Transitions	
					Lower level	Upper Level
FeII	321.8	2.4e+06	73 43.346	104 09.618	$3d^6(^1G2)4p$	$3d^6(^3H)4d$
FeI	357.38	2.41e+06	19 390.168	47 363.376	$3d^64s^2$	$3d^6(^3G)4s4p(^3P°)$
FeI	373.53235	2.70e+07	24338.76 7	50 475.288	$3d^6(^5D)4s4p(^3P°)$	$3d^6(^1G2)4s4p(^3P°)$
FeI	382.54025	6.47e+05	18 378.186	44 511.812	$3d^64s^2$	$3d^7(^4P)4p$
FeI	388.70480	3.52e+06	7 376.764	33 095.941	$3d^7(^4F)4s$	$3d^7(^4F)4p$
FeI	393.11170	4.8e+06	26 339.696	51 770.557	$3d^6(^5D)4s4p(^3P°)$	$3d^6(^5D)4s\ (^4D)5s$
FeI	399.80525	5.70e+06	21 715.732	46 720.842	$3d^7(^2G)4s$	$3d^7(^4P)4p$
FeI	406.53809	1.7e+07	27 666.348	52 257.346	$3d^6(^5D)4s4p(^3P°)$	$3d^6(^5D)4s\ (^4D)5s$
OII	495.5705	1.81e+07	214 229.671	234 402.797	$2s^22p^2(^3P)3p$	$2s^22p^2(^3P)3d$
FeI	518.68670	2.64e+07	84 424.422	103 698.515	$3d^6(^5D)4d$	$3d^6(^5D_2)4f$
FeI	526.33059	6.36e+06	26 339.696	45 333.875	$3d^6(^5D)4s4p(^3P°)$	$3d^6(^5D)4s\ (^6D)5s$
FeII	589.8114	5.4e+05	54 275.649	72 169.004	$3d^54s^2$	$3d^6(^3D)4p$
OIII	599.528	6.18e+05	377 562.31	394 197.9	$2s^22p(^2P°)4d$	$2s2p^2(^2D)3s$
FeII	601.78830	3.1e+05	63 272.981	79 885.523	$3d^6(^3F2)4p$	$3d^6(^5D)5s$
FeI	612.02490	2.12e+01	7 376.764	23 711.456	$3d^7(^4F)4s$	$3d^6(^5D)4s4p(^3P°)$
FeI	616.35441	8.44e+03	17 726.988	33 946.933	$3d^7(^4P)4s$	$3d^6(^5D)4s4p(^3P°)$
OII	649.5802	1.48e+06	232 796.298	248 186.64	$2s^22p^2(^3P)3d$	$2s^22p^2(^3P)4p$

Boltzmann plot requires peaks that originated from the ionization stage and the same atomic species. We choose five peaks for Fe_2O_3 at (321.8, 373.57, 388.7 and 601.37) nm as shown in Fig. 4. We get these peaks after incident laser on target in air Fig. 1(b) and choose the energies of transition probabilities, high levels and statistical weights for element Fe_2O_3 have been obtained from (NIST) [22], where T_e equals to the invert of the slope of the fitting line according to Eq. (1). The fitting lines R^2 is a statistical coefficient indicating the goodness of the linear fit which takes a value between (0.8, 0.9) as shown in Fig. 5. Using Stark broadening Eq. (2) to determine the n_e , where the spectral lines of plasma electrons result from collisions with charged species.

Table 2 shows surfaces of Fe_2O_3. We found it through the values of parameters (T_e, *FWHM*, *ne*, f_p, λ_D, and N_d), where f_p and N_D at different laser pulse energies (600- 900) mJ calculated though the FWHM methods appear from Table 2 and Fig. 6, the plasma generated dependent on the plasma conditions. It shows that (*ne*, f_p) increases with laser energy.

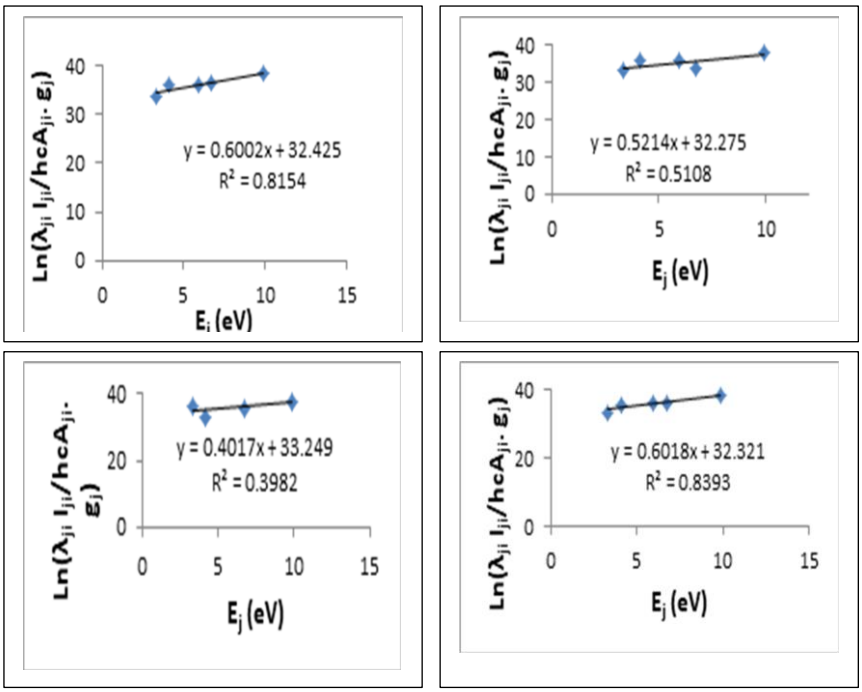

Fig. 5. Boltzman plot for Fe_2O_3 target with different laser energies in the air.

Table 2. Plasma parameters (T_e, n_e, f_p, λ_D, and N_d) for the Iron Fe_2O_3 with different laser energies (600-900).

E (mJ)	T_e (eV)	$FWHM$	$n_e \times 10^{17}$ (cm^{-3})	f_p (Hz)$\times 10^{12}$	$\lambda_D \times 10^{-5}$(cm)	$N_d\,10^3$
900	1.660	1.350	10.13	9.036	0.951	3.652
800	1.660	1.340	10.05	9.002	0.951	3.621
700	1.900	1.320	9.90	8.935	1.025	4.468
600	2.400	1.300	9.75	8.867	1.161	6.391

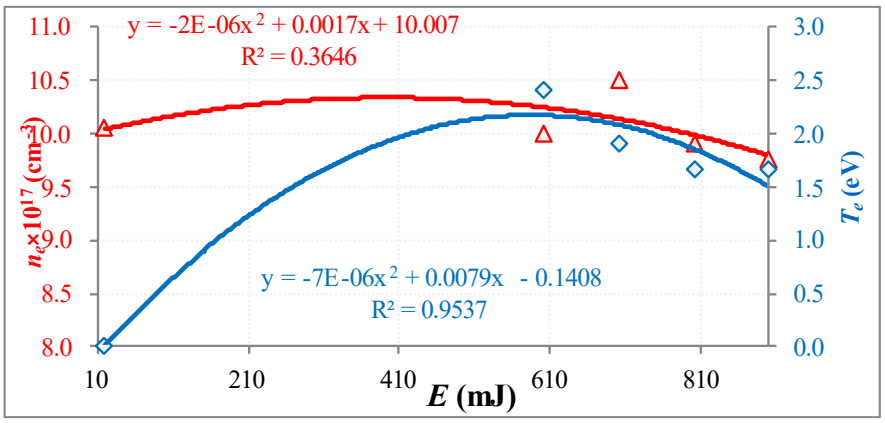

Fig. 6. the variation of (T_e) and (n_e) versus the laser energy(600, 700, 800, and 900) for Fe_2O_3.

4. Applications

Staphylococcus aureus is a microorganism that live in the skin and mucose membranes of humans as normal flora, it is a gram-positive cocci, gold-coloured, pairs and cluster, it's very common in hospitals wherever patients with open wounds and weakened immune systems. They are recognized as foodborne and clinical pathogen, inhabiting the skin, skin glands and mucous membranes of humans (Matthew, 2012), these bacteria have troublesome in hospitals, prisons and nursing homes, where patients with open wounds, invasive devices, and weakened immune systems. It has ability to biofilm forming as another human pathogens that causes diseases, ranging from minor skin lesions to dangerous deep tissue harm, and general infections like respiratory disease, carditis, and toxin syndromes [23].

Acinetobacter baumannii is a Gram-negative, non-motile, obligate aerobic coccobacilli that is commonly found in soil, water, sewage, and in healthcare settings ,it is one of the most important pathogens causing hospital-acquired infections (nosocomial infections), particularly in intensive care units (ICUs) Acinetobacter baumannii is the causative agent of wide range of infections including sever bacteraemia, septicaemia ventilator-associated pneumonia , wound infections meningitis ,endocarditis , skin and soft tissue infections urinary tract and catheter-related infections, osteomyelitis, ocular infections, and many other hospital and ICU-acquired illnesses especially in patients with impaired host defences [23].

5. Well Diffusion - Method

Different nano particle liquid plasma energy as shown in Fig. 7 used to screen for their inhibitory activities against human pathogenic bacteria (Acinetobacter baumannii and Staphylococcus aureus). This procedure must be used agar well diffusion-method. Plates were prepared by spreading 105 cfu/ml culture broth of indicator microorganisms isolate on surface nutrient agar surface. The agar plates were left for about 15 min. before aseptically dispensing the 50 µl of Fe_2O_3 solution into the agar wells already bored in the agar plates. The plates were then incubated at 37 °C for (18-24) hours. Zones of inhibition were measured and recorded in millimetres diameter as shown in Fig. 8.

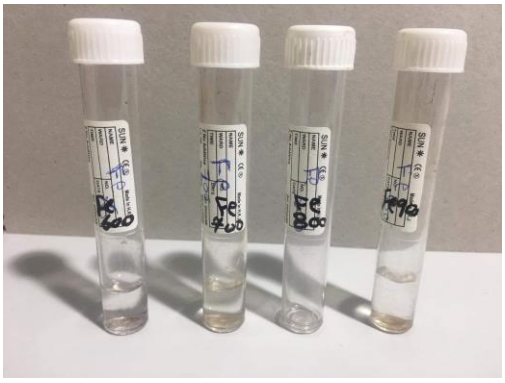

Fig.7. Fe_2O_3 nano particle liquid in different plasma energy (600-900) mJ.

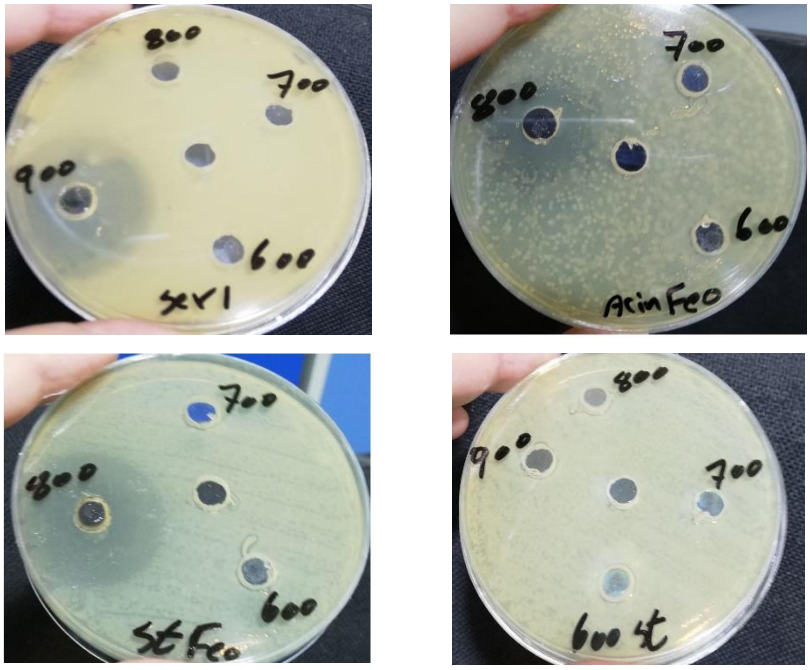

Fig. 8. Effect of Fe_2O_3 plasma energy on the against *S*, aureus and Acinetobacter baumannii.

6. Conclusions

Laser-induced Plasma spectroscopy (LIPS) technique has been applied to study the emission of plasma from target, and the analysis of Fe_2O_3 plasma plume using the fundamental (1064 nm) Nd: YAG laser. Also study the plume intensity, electron temperature (Te), and electron density (ne) of plasma plume are determined at different Nd: YAG laser energies (600-900) nm. It is observed in case of iron the laser energy and the electron temperature increase with it and the highest peak of Fe_2O_3 arrives at 62672.95.

This research shows high effect of Fe_2O_3 at 800 against S, aureus with inhibition zone 30 (mm) and 23(mm) on Acinetobacter baumannii while no effect at 700, 600 on both type of bacteria. Their antimicrobial effect is due to blockage of respiratory enzyme pathways, the cell wall, inhibition the protein synthesis, may be effect on the alteration of microbial DNA and outer membrane permeability.

Acknowledgments

The author is deeply grateful to the Prof. Dr. Khalid A. Ahmed, and Lab. of plasma in the department of Physics and Lab of biology/ College of science/ Mustansiriyah University.

References

1. Apaydin, E.; and Celik, M.; (2019). Investigation of the plasma parameters of a laboratory argon plasma source using a collisional radiative model with the

comparison of experimental and simulated spectra. *Spectrochimica Acta Part B: Atomic Spectroscopy*, 160, 105673.

2. Fantz, U.; (2006). Basic of plasma spectroscopy. *Plasma Sources Science and Technology*, 15(4), S137-S147.
3. Naser, D.K.; Abbas, A.K.; and Aadim, K.A. (2020). Zeta potential of Ag, Cu, ZnO, CdO and Sn Nanoparticles prepared by pulse laser ablation in liquid environment. *Iraqi Journal of Science*, 61(10), 2570-2581.
4. Boloukil, N.; Hsing, J.-H.; Li, C.; and Yang, Y.-Z. (2019). Emission spectroscopic characterization of a helium atmospheric pressure plasma jet with various mixtures of argon gas in the presence and the absence of de-ionized water as a target. *Plasma*, 2(3), 283-293.
5. Pasquini, C.; Cortez J.; Silva, L.M.C.; and Gonzaga, B. (2007). Laser induced breakdown spectroscopy. *Journal of the Brazilian Chemistry Society*, 18(3), 463-512.
6. Putri, N.R.E.; Firdausi, S.I..; Najmina, M.; Amelia, S.; Timotius, D.; Kusumastuti, Y.; and Petrus, H.T.B.M. (2020). Effect of sonication time and particle size for synthesis of magnetic anoparticle from local iron sand. *Journal of Engineering Science and Technology* (*JESTEC*), 15(2), 894-904.
7. Rivas, D.E.; Borot, A.; Cardenas, D.E.; Marcus, G.; Gu, X.; Herrmann, D.; Xu, J.; Tan, J.; Kormin, D.; Ma, G.; Dallari, W.; Tsakiris, G.D.; Földes, I.B.; Chou, S.-w.; Weidman, M.; Bergues, B.; Wittmann, T.; Schröder, H.; Tzallas, P.; Charalambidis, D.; Razskazovskaya, O.; Pervak, V.; Krausz, F.; and Veisz, L. (2017). Next generation driver for attosecond and laser-plasma physics. *Scientific Reports*, 7, 5224.
8. Pavone, B.A.; Svensson, J.; Kwak, S.; Brix, M.; Wolf, R.; and JET Contributors (2020). Neural network approximated Bayesian inference of edge electron density profiles at JET. *Plasma Physics and Controlled Fusion*, 62(4), 045019.
9. Shaikh, N.M.; Tao, Y.; Burdt, R.A.; Yuspeh, S.; Amin, N.; and Tillack M.S. (2010). Spectroscopic studies of tin plasma using laser induced breakdown spectroscopy. *Journal of Physics: Conference Series*, 244, 042005.
10. Barton, L.L. (2005). *Structural and functional relationships in prokaryotes*. New York, Springer.
11. Harilal, S.S.; O'Shay, B.; and Tillack, M.S. (2005). Spectroscopic characterization of laser-induced tin plasma. *Journal of Applied Physics*, 98(1), 013306.
12. Dabagh, S.; Chaudhary, K.; Haider, Z.; and Ali, J. (2018). Study of structural phase transformation and hysteresis behavior of inverse-spinel α-ferrite nanoparticles synthesized by co-precipitation method. *Results in Physics*, 8, 93-98.
13. Harilal, S. S.; Bindhu, C.V.; Isaac, R.C.; Nampoori, V.P.N.; and Vallabhana, C.P.G. (1997). Electron density and temperature measurements in a laser produced carbon plasma. *Journal of Applied Physics*, 82(5), 2140-2146.
14. Essa, M.A; and Aadim K.A. (2019). Spectroscopic studying of plasma parameters for SnO2 doped ZnO prepared by pulse Nd:YAG laser deposition. *Iraqi Journal of Physics*, 17(42), 125-135.

15. Khalaf, M.A.; Ahmed, B. M.; and Aadim, K.A. (2020). Spectroscopic analysis of CdO1-X: SnX plasma produced by Nd:YAG Laser. *Iraqi Journal of Science*, 61(7), 1665-1671.
16. Unnikrishnan, V.K.; Alti, K.; Kartha,V.B.; Santhosh, C.; Gupta, G.P.; and Suri, B.M. (2010). Measurements of plasma temperature and electron density in laser-induced copper plasma by time-resolved spectroscopy of neutral atom and ion emissions. *Pramana - Journal of Physics*, 74(6). 983-993.
17. Abbas, A.K.; and Muslim, S.I. (2017). Measurement the parameters of cadmium oxide plasma induced by laser. *International Journal of Recent Research and Applied Studies*, 4(10), 66-72.
18. Ahmed, B.M.; Ahmed, K.A., and Ahmed, R.K. (2016). Energy loss of correlated ions in dense. *Plasma, Electronic Materials Letters*, 12(3), 419-424
19. Hussain, A.A.-K.; and Naama, Razzaq, A.A.A. (2016). Plasma characteristics of Ag:Al alloy produced by fundamental and second harmonic frequencies of Nd:YAG. Laser. *Iraqi Journal of Physics*, 14(31), 205-214.
20. Harry, J.E. (2010). *Introduction to Plasma Technology: Science, Engineering and Applications*. Wiley-VCH Verlag GmbH & Co. KGaA, Weinheim
21. National Institute of Standards and Technology (NIST) atomic spectra database (version 5). Retrieved October 5, 2020, from http://www.nist.gov/pml/data/asd.cfm.
22. Melke, P.; Sahlin, P.; Levchenko, A.; and Jonsson H. (2010). A cell-based model for quorum sensing in heterogeneous bacterial colonies. *PLoS. Computational Biology*, 6(6):1000819.
23. Munoz-Price, L.S.; Zembower, T.P.; Schreckenberger, S.; Lavin, P.; Welbel, M.A.; Vais, S.; Baig, D.M.; Mohapatra S.; Quinn, J.P.; and Weinstein, R.A. (2010). Clinical outcomes of carbapenem-resistant Acinetobacter baumannii bloodstream infections: study of a 2-state monoclonal outbreak. *Infection Control & Hospital Epidemiology*, 31(10), 1057-1062.